JPRS-UPM-91-005
1 JULY 1991

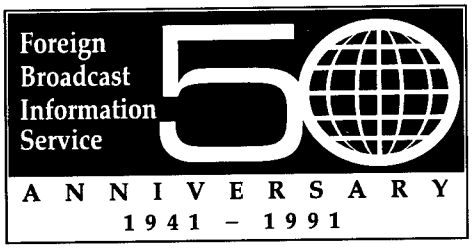

JPRS Report

Science & Technology

USSR: Physics & Mathematics

Science & Technology
USSR: Physics & Mathematics

JPRS-UPM-91-005 *01 July 1991*

CONTENTS

Optics, Spectroscopy

Plasma Physics

Superconductivity

Theoretical Physics

Differential Equations

Velocity Dispersion of Longitudinal Ultrasonic Waves in NaCl

917J0065C Leningrad FIZIKA TVERDOGO TELA in Russian Vol 32 No 11, Nov 90 pp 3362-3365

[Article by A. M. Petchenko]

UDC 548.4:534.8

[Abstract] Dispersion of elastic waves in crystals under strain was studied experimentally in [100]-oriented NaCl single crystals, ultrasonic waves propagating through them in that direction. The crystals, 30 mm long and 20 mm square in cross-section, had retained impurities and glissile dislocations after annealing. The frequency of longitudinal ultrasonic waves was varied over the 7.5 - 217.5 MHz range, each frequency being recorded accurately within 0.08 - 0.15 percent. Measurements were made by the echo pulse method at room temperature, with a crystal first undeformed, and then after it was deformed, by compression at room temperature to residual strains from 0.2 percent to 1.0 percent. The dispersion range was found to widen and shift toward lower frequencies as the crystal strain increased, this shift however becoming smaller with increasing crystal strain. Compression was not extended to still larger residual strains, which would have shortened the dislocation loops and eventually reversed the shift of the widening dispersion range toward higher frequencies, because excessive attendant damping of ultrasonic waves would degrade the accuracy of their velocity readings. Instead, the length of dislocation segments was reduced by treatment of a crystal having a 0.5 percent residual strain with a 300 R dose of x-rays so that the corresponding dispersion curve shifted closer to that for an undeformed crystal. Measurements were made within 20 min after a crystal had been deformed so as to eliminate the effect of aging. These measurements have revealed how the velocity of ultrasonic waves depends on their frequency at various levels of crystal strain, this dependence being linear in an undeformed crystal ($v = 4762$ m/s at $f = 217.5$ MHz), and how it depends on the crystal strain at various frequencies. The velocity decrement $\Delta v(f)$ was found to be largest in a crystal with a 1 percent residual strain, smallest in one with 0.5 percent residual strain and treated with x-rays. A correlation between the experiment and theory has been established on the basis of the frequency dependence of the relative C_{11} modulus decrement, measurements agreeing closely with calculations based on an exponential distribution of dislocation loop lengths. According to the results of this study, the velocity dispersion of ultrasonic waves due to their scattering in a crystal depends largely on the density of glissile dislocations. Such dislocations were found to scatter ultrasonic waves of frequencies up to 200 MHz. The velocity dispersion of ultrasonic waves, moreover, is influenced by and depends on the crystal strain. The dispersion range was found to widen with increasing strain, shifting first decreasingly toward lower frequencies and then eventually toward higher frequencies. Figures 3; references 12.

Study of Shock Waves From Annular Surface Discharge and Their Interaction With Stationary Sphere

917J0070C Leningrad ZHURNAL TEKHNICHESKOY FIZIKI in Russian Vol 60 No 12, Dec 90 pp 12-146

[Article by A. P. Bedin, A. B. Safonov, and M. N. Troitskiy, Institute of Engineering Physics imeni A. F. Ioffe, USSR Academy of Sciences, Leningrad]

[Abstract] An experimental study of toroidal shock waves from an annular surface discharge was made, such waves eventually collapsing and forming conical funnels with a Mach disk. Annular surface discharge over an array of 24 disk electrodes 11 mm in diameter forming a ring 100 mm in diameter was produced by a 0.5 μF capacitor charged to 30 kV and discharging through a high-voltage cable bent into a circular loop around the electrodes. The waveform of the discharge current was a damped sinusoid. The discharge time was about 15 μs in air under atmospheric pressure at 290 K temperature and the velocity of shock waves thus generated was 410 m/s. Axially collapsing and transversely collapsing ones were photographed while their respective axial and radial velocities as well as the velocity of the Mach disk shifting in the process were measured, as functions of time and as functions of the longitudinal coordinate in the direction of shock wave propagation. In the second part of the experiment funnels formed by collapsing toroidal shock waves were made to strike a stationary sphere 27 mm in diameter. These tests were performed with 77 J and 225 J discharge energy. The distance from the stagnation point on the sphere to the plane of the active annular electrode surface was varied from 0 to 100 mm so as to establish the dependence of the interaction energy on that distance. The interaction energy was found to peak to a maximum of about 50 MJ when that distance was 20 mm, as compared with the 2-3 MJ peak in the case of a sphere 30 mm away from a rectilinear discharge. The interaction energy was also measured as a function of time over a 200 μs period from the instant of incidence, the initially higher velocity of the shifting Mach disk having, within this time, already leveled down to the 410 m/s velocity of the shock wave. An incident shock was found to maximally reflect by the sphere at 45° angles from the axis. Figures 7; references 5.

Acoustic 'Laser'

917J0076A Moscow AKUSTICHESKIY ZHURNAL in Russian Vol 37 No 1, Jan-Feb 91 pp 123-129

[Article by A. N. Kotyusov, B. Ye. Nemtsov, Radiophysics Scientific Research Institute]

UDC 53.01+551.510:534.222.1

[Abstract] The coherent mechanism of sound generation during the water vapor condensation and the accompanying amplification effect are discussed. To verify the phenomenon experimentally, a Helmholtz resonator (RG) filled with supersaturated steam is considered and acoustic vibrations in this RG are examined. The RG consists of a vessel

with a narrow neck through which it communicates with the ambient medium. Condensation is more intensive than evaporation in the RG, so heat is released in the system; a portion of this energy is expended to amplify acoustic vibrations. An integrodifferential which takes into account the processes of condensation and heat transfer from condensation centers in the gas is derived. An analysis of the approximate solution demonstrates that steady-state vibrations are formed in the RG whose amplitude and frequency depend on resonator and internal medium parameters. The possibility of verifying the above phenomenon experimentally is discussed. The pressure level in the stimulated wave is estimated. These estimates show that the proposed sound wave stimulation mechanism may be rather effective in lab conditions and may be used for generating powerful acoustic vibrations. The authors are grateful to Ye. Yu. Kuznetsov for making numerical calculations and giving useful advice. References 12: 5 Russian, 7 Western.

Magnon Drag of Conduction Electrons in Magnetic Semiconductors in Field of Strong Electromagnetic Wave

917J0065B Leningrad FIZIKA TVERDOGO TELA in Russian Vol 32 No 11, Nov 90 pp 3206-3209

[Article by V. P. Gnedkov, V. P. Seminozhenko, V. L. Sobolev, and D. F. Fil, Scientific-Industrial Association "Monokristalreaktiv" (Single Crystal Reagent)

UDC 538.22

[Abstract] Interaction of conduction electrons and localized magnetic moments in magnetic semiconductors, manifested in a drag of electrons by spin waves owing to s-d exchange interaction, is analyzed when this drag occurs in the presence of a strong electromagnetic wave whose field quanta participate in the attendant electron-magnon interaction. The current density due to drag by a coherent spin wave with a magnon distribution of the $N_k = N_k\delta(k - q)$ kind (q - spinwave vector) is calculated separately for ferromagnetic and antiferromagnetic semiconductors with wide conduction bands in a high-frequency, high-intensity electric field of an externally generated electromagnetic wave, assuming that $(T,\varepsilon_F,\varepsilon_q) < \Delta/2$ (T - temperature, ε_F - Fermi electron energy, $\varepsilon_q = q^2/2m$, m - electron mass) and ignoring the spin splitting of the conduction band in antiferromagnetic semiconductors. The analytical expressions derived on this basis indicate that magnon drag of conduction electrons is possible with or without an electromagnetic wave generating an external electric field, but not without such an electric field in degenerate ones with $\varepsilon_F < \Delta/2$, while in degenerate antiferromagnetic semiconductors as well as in nondegenerate ones it is possible with or without such an external electric field. The ratio of the calculated potential difference produced by a spin wave to its measurable input power is estimated numerically for ferromagnetic and antiferromagnetic semiconductors at a temperature $T \approx 10$ K, with an s-d exchange constant $J_{s-d} = 0.1$ eV, a volume of the unit cell $V_0 \approx 10^{-22}$ cm^3, and a magnon temperature $T_N \approx 150$ K. References 8.

On Stochastization of Planar-Parallel Perfect Fluid Flows

917J0075B Moscow VESTNIK MOSKOVSKOGO UNIVERSITETA: MATEMATIKA, MEKHANIKA in Russian No 1, Jan-Feb 91 pp 72-76

[Article by V. V. Kozlov]

UDC 517.9

[Abstract] Planar-parallel flows of an homogeneous ideal fluid in a potential field of forces are described by a system of equations whose variables are the fluid particles' velocity components, pressure, constant density, and potential energy of external mass forces. It is shown that a typical harmonic disturbance of the constant direction of a steady state velocity field leads to a stochastization of the ideal fluid flow. A problem of a pair of vortices is considered and the results of numerical calculations of the disturbed flow excited by a pair of vortices of opposite intensities are cited. The separatrix splitting and the formation of stochastic layers are illustrated. Numerical calculations also show that in a simpler problem of disturbing the velocity field of an isolated vortex, generation of stochastic layers is also observed. The author is grateful to A. V. Borisov for help with numerical calculations. References 4; figures 1.

Stabilization of Beats and Alternating Optical Nonreciprocity During Nonstationary Self-Diffraction of Self-Bias Waves in Active Medium of Solid-State Ring Laser

917J0069A Moscow KVANTOVAYA ELEKTRONIKA in Russian Vol 18 No 1, Jan 91 pp 76-78

[Article by N. V. Kravtsov, S. V. Parfenov, and A. N. Shelayev, Scientific Research Institute of Nuclear Physics at Moscow State University imeni M. V. Lomonosov]

UDC 621.378.3.826.038.825

[Abstract] An experimental study of a rotating YAG:Nd^{3+} ring laser with a uniformly broadened amplification line and with self-bias waves was made, such waves being generated as a result of transient acoustooptic feedback during Doppler modulation of the optical carrier frequency of ultrashort self-bias pulses. They separate the frequencies of counterpropagating waves in such a ring laser and thus eliminate competition of these waves by converting it into beats. The active medium of the laser in the main cavity branch between two plane mirrors was pumped by a krypton-arc lamp and emitted 1.064 μm radiation with mode locking. Rotation of the laser crystal and use of a nonreciprocal Faraday cell between the other two plane mirrors in the feedback branch ensured a larger than 1 MHz absolute difference between the natural frequencies of the optical cavity for counterpropagating waves. Mode locking was effected by an acoustooptic device in the feedback branch, a (Y+36°)-cut $LiNbO_3$ crystal with a 125 MHz first critical frequency with a standing 47.68 μm ultrasonic wave in an acoustooptic wave guide made of fused quartz. This device operated in the Bragg diffraction mode and modulated the radiation losses in the ring laser at the intermodal beat frequency, which was approximately c/L = 250 MHz and thus twice its first critical, within an approximately 2.3 cm long interaction space. High beat stability, i.e., a very stable difference between the frequencies of counterpropagating waves was attained by use of only one self-bias wave, namely the diffracted beam of rays, and by use of that diffracted beam for resonant feedback, this beam returning upon reflection by an oscillating mirror or prism with a 180° quasi-reversed wavefront. The results of this experiment indicate that it is feasible to effectively stabilize 10-100 kHz beat frequencies in such a ring laser within 10 Hz or less for a period of 10 s. Figures 2; references 5.

Spectrum Compression and Phase Conjugation of KrF Excimer Laser Radiation

917J0069B Moscow KVANTOVAYA ELEKTRONIKA in Russian Vol 18 No 1, Jan 91 pp 89-90

[Article by S. S. Alimpiyev, V. S. Bukreyev, S. K. Vartapetov, I. A. Veselovskiy, V. I. Kusakin, S. V. Likhanskiy, and A. Z. Obidin, Institute of General Physics, USSR Academy of Sciences, Moscow]

UDC 621.373.826.038.823

[Abstract] A set of series 1701 commercial KrF excimer lasers with electrical discharge pumping by pulses of approximately 20 ns duration was assembled for an experimental study of both phase conjugation of radiation during its stimulated scattering in gaseous SF_6 or in liquid C_6H_{14} and spectrum compression by a diffraction grating. The optimum active medium of these lasers, occupying a 1x2x50 cm^3 volume, is an F_2Kr:Ne = 5:70:1600 mm Hg mixture capable of radiation emission in pulses of about 200 mJ energy at the maximum repetition rate of 50 Hz. Radiation from the master laser-oscillator was injected into a regenerative laser-amplifier with a 10x magnifying telescopic cavity. The exit mirror of this cavity was a meniscus mirror with a reflecting layer 2.5 mm in diameter deposited on its surface. The laser-amplifier emitted radiation without widening it spectrum, in pulses of 140 mJ energy within a beam whose divergence did not exceed 0.1 mrad. A diffraction grating with 2400 lines/mm at an 84° angle for grazing incidence and two Fabry-Perot solid state etalons, with 1 mm and 10 mm bases respectively, were used for compressing the radiation emission spectrum of the laser-oscillator. As the stimulated-scattering medium was first used gaseous SF_6 under a pressure of 10 atm, this substance having excellent nonlinearity characteristics and being transparent for 248 nm radiation. The pump pulse and emission pulse parameters were measured with the aid of a beam splitter diverting some of the radiation. The energy characteristics of radiation were measured with an IMO-2N calorimeter. The time characteristics of radiation pulses were recorded by an FK-22 photocell with a 0.6 ns time resolution. The widths of both pump and scattering spectra as well as the Brillouin frequency shift were measured with a Fabry-Perot solid state etalon having a 28 mm base. This experiment yielded a pulse compression to 1.5 ns and a spectrum compression to 0.02 cm^{-1} without a Brillouin frequency shift, indicating stimulated scattering by the SF_6 Mandelshtam-Brillouin mirror. An analogous experiment with liquid n-hexane as stimulated-scattering medium yielded a pulse compression to only 2.5 ns with a not larger than 0.02 cm^{-1} and thus negligible rather than the nominal 0.3 cm^{-1} Brillouin frequency shift, indicating stimulated temperature rather than Mandelshtam-Brillouin scattering in this medium. Figures 3; references 6.

Formation and Propagation of Stationary Laser Pulses in Media With Both Third-Order and Fifth-Order Nonlinearities

917J0069C Moscow KVANTOVAYA ELEKTRONIKA in Russian Vol 18 No 1, Jan 91 pp 104-106

[Article by B. S. Azimov, M. M. Saratov, and A. P. Sukhorukov, Moscow State University imeni M. V. Lomonosov]

UDC 621.373.826

[Abstract] Formation of laser pulses in media with quintic as well as cubic nonlinearities and their propagation through such media in quasi-plane wave packets with phase modulation in time are analyzed theoretically on the basis of the one-dimensional nonlinear Schroedinger equation, to which there has been added the $2i\delta A/\zeta - \delta^2 A/\delta t^2 = \alpha|A|^2A + \beta|A|^4A$ term in the expansion of the nonlinear polarization vector (A - momentum matrix, z - coordinate in the direction of propagation, t - tracking time), $\alpha = L_d/L_{nl}^a$, $\beta = L_d/L_{nl}^b$,(L_d - dispersion length, L_{nl} - nonlinearity length with superscripts "a" and "b" referring to cubic nonlinearity alone and to quintic nonlinearity alone, respectively). The steady-state solutions are compared with the well known solution for a cubic nonlinearity alone ($\beta = 0$). In the case of $\beta > 0$ the steady-state solutions are intermediate between a fundamental soliton and a "soliton on quintic nonlinearity", their profiles in time depending on the propagation constant Γ as the form factor and with $R = \alpha^2/4 + 4\beta\Gamma^2 > 0$. In the case of $\beta < 0$ there are two kinds of solutions: 1) when $\alpha < 0$, then the dispersion and both nonlinearities cooperate so that a wave packet becomes diffuse and steady waves except unmodulated ones cannot form; 2) when $\alpha < 0$, then the nonlinearity of the medium is saturated so that another family of solutions is possible as long as $R \geq 0$ and their profile depends again on the propagation constant Γ which, however, can now be varied from 0 to some Γ_{max} only. All steady-state solutions are tested for stability, after transient-state solutions have been demonstrated on the evolution of a Gaussian wave packet and its envelope, whereupon the conditions for formation of corresponding pulses under arbitrary initial conditions are established by taking into account the effect of quintic nonlinearity with $\beta > 0$ when also $\alpha > 0$. Figures 4; references 6.

Phase Effects in Passive Nonlinear Optical Cavities

917J0069D Moscow KVANTOVAYA ELEKTRONIKA in Russian Vol 18 No 1, Jan 91 pp 121-126

[Article by M. A. Vorontsov and K. V. Shishakov, Moscow State University imeni M. V. Lomonosov]

UDC 535.416.3

[Abstract] Phase effects in passive nonlinear optical ring cavities are analyzed theoretically on the basis of a physical model which includes a regenerative laser-amplifier followed by a phase screen and then a thin Kerr cell in the main cavity branch, between the front mirror and the exit mirror, and another phase screen between the other two mirrors in the feedback branch. Nonlinear phase modulation in such a cavity is described by the corresponding relaxation equation for the complex field amplitude before the Kerr cell. The steady-state solution to this equation indicates suppression of phase distortions by a process similar to phase conjugation, diffraction evidently not playing a role here. Phase modulation and adaptive phase control by the phase screen in the feedback branch of such a cavity are considered next, now the condition for suppression of phase distortions being that the distribution of modulating intensity be proportional to the distribution of phase nonuniformity with a negative sign. The wavefront, i.e., the phase profile on the exit side is determined accordingly. Local transverse interactions induced by diffusion and weak diffraction are then evaluated, diffusion effects in the nonlinear Kerr medium on the basis of the appropriately modified equation of nonlinear phase modulation and diffraction effects in the feedback branch on the basis of the parabolic diffraction equation. Both diffusion and diffraction lower the Strehl number and thus weaken the suppression of phase distortions. Numerical estimates confirm that compensation by aperture scanning is more effective than self-compensation. Figures 7; references 14.

Self-Sustaining Volume Discharge After Preionization by Ultraviolet Radiation or Soft X-Rays

917J0070B Leningrad ZHURNAL TEKHNICHESKOY FIZIKI in Russian Vol 60 No 12, Dec 90 pp 43-48

[Article by S. L. Kulakov, A. A. Kuchinskiy, A. G. Maslennikov, Yu. V. Rybin, V. A. Smirnov, V. P. Tomashevich, and I. V. Shestakov, Leningrad Polytechnic Institute imeni M. I. Kalinin]

[Abstract] An experimental study of self-sustaining volume discharge in a long interelectrode gap of a pulsed CO_2-laser with electrical discharge pumping was made, for a comparative evaluation of preionization by ultraviolet radiation and soft x-rays. The apparatus consisted of a flat solid anode and a convex cathode, the latter with a window in the form of a brass grid at the center for extraction of the preionizing radiation. The gap between the electrodes was 22 cm long and the volume of the discharge space was 40 dm^3. Discharge was produced by a 4-stage Arkadyev-Marx generator of voltage pulses with an effective capacitance of 0.125 μF and with an external shunt capacitance for varying the pulse rise time over the 0.060 - 2.5 μs range, the pulse amplitude being varied over the 50-70 kV range and the specific energy input for discharge varied correspondingly over the 60-125 J/dm^3 range. Ultraviolet preionization was provided by an array of linear multigap radiators with a spark density of about 0.5 cm^2, powered by a 0.5 μF 40 kV capacitive energy storage. Preionization by x-rays was provided by drift of electrons and attendant sliding nanosecond discharge in the plasma of a convex slab of acrylic glass lining the inside of the cathode and emitting soft x-rays, upon excitation by a generator of high-voltage nanosecond pulses in the form of a double-strip

pulse shaping line with a controlled nitrogen-filled (pressure 6 atm) discharger triode acting as switch. The active medium of the laser in this experiment was a CO_2N_2:He = 1:1:8 mixture under atmospheric pressure. During each test, the voltage across the discharge voltage and current were measured. The initial photoelectron concentration determined from photocurrent readings. The effective energy of x-rays was estimated with the aid ofaluminum foils. The discharge was also photographed. The laser emission characteristics were measured inside a 3 m wide optical cavity between a flat germanium disk (diameter 190 mm) and a convex copper mirror (diameter 350 mm, radius of curvature 12 m), this cavity occupying 45 percent of the active discharge space. A part of the radiation was reflected by a BaF_2 plate and measured with an array of calorimeters. The data reveal that preionization by soft x-rays with an energy input of 60-125 J/dm^3 and a short rise time of voltage pulses facilitated formation of a uniform discharge in that CO_2:N_2:He = 1:1:8 mixture. Preionization by ultraviolet radiation with an energy input up to 125 J/dm^3 did not result in a stable discharge, unless the rise time of voltage pulses was lengthened to 400-500 ns, and the discharge was not as uniform in any case. It has also been found that for preionization by soft x-rays triethylamine is not suitable as easily ionized material, because of plasmochemical reactions into which it enters with the active laser medium. Figures 5; references 15.

Tunnel Ionization of Potassium and Xenon Atoms in Intense CO_2 Laser Field

917J0080A Moscow ZHURNAL EKSPERIMENTALNOY I TEORETICHESKOY FIZIKI in Russian Vol 99 No 2, Feb 91 pp 481-487

[Article by W. Xiong, S. L. Chin, Optics, Photonics, and Laser Center at the Laval University, Quebec, Canada]

[Abstract] Experimental data on the ion yield and electron liberation during the tunnel ionization of two completely different atoms—potassium and xenon—are compared to various versions of Ammosov's, Delone's, and Kraynov's tunnel effect theory. Two types of experiments were performed. In one, 2 ns long pulses of a CO_2 laser at λ = 10.6μm were used whereby the effusion potassium atom beam was intersected by a laser beam, resulting in the formation of K^+ ions and electrons. In the other, 1.1 ns long CO_2 laser pulses were used to ionize stationary xenon atom gas. A well known transit time and retarding potential-based detection technique was used. The experimental results are consistent with theoretical data. A need for further investigation is noted. The authors are grateful to S. Lagach for help with experiments and to S. Augst, D. Meyerhofer, P. B. Corkum, J. Mainfre, J. Eberly, F. Yergeau, and P. Lavigne for useful discussions. References 12: 2 Russian, 10 Western; figures 6.

Self-Excited Oscillation of Electron Beam in Accelerating Structure of Linear Backward-Wave Accelerator

917J0063A Leningrad PISMA V ZHURNAL TEKHNICHESKOY FIZIKI in Russian Vol 17 No 1, 12 Jan 91 pp 75-78

[Article by V. V. Kozlyuk, Institute of Chemical Kinetics and Combustion, Siberian Department, USSR Academy of Sciences]

[Abstract] An experiment with an electron beams in a linear backward-wave accelerator has revealed self-excited oscillations of such a beam in the accelerating structure. The accelerating structure in this experiment was 0.7 m long. The parameters of the fundamental accelerating electric field harmonic were a 1.5 ratio of initial phase velocity to final phase velocity in the direction of high-frequency power flow and a 8,000 V/(m.$W^{1/2}$) mean, over the length of the structure, ratio of voltage amplitude to square root of high-frequency output power. The total attenuation of the electromagnetic wave was $\alpha = -3$ dB. The focusing magnetic field was made sufficiently strong so as to ensure that the beam current would not precipitate more than 10-20 percent of all electrons on the channel walls. Both beam injector on the input side and the beam probing apparatus on the output side where the longitudinal magnetic field had dropped to 70 percent of the focusing magnetic field. Beam oscillations were recorded with a VEU-1 secondary-electron multiplier in a guard ring at an adjustable retarding higher than the injection potential. Nondecaying self-excited oscillations with a distinct repetition period of about 120 ns and not more than 60 percent amplitude modulation were detected when the beam power P_b and the high-frequency input power P_{hf} came close to being equal: $P_b \approx P_{hf}/10^{0.1\alpha}$. Calculations based on a theoretical analysis of this phenomenon yield a pulse repetition period of 108 ns. Figures 2; references 7.

High-Speed Scintillator Crystals for Nuclear Radiation Detectors

917J0064B Leningrad PISMA V ZHURNAL TEKHNICHESKOY FIZIKI in Russian Vol 16 No 22, 26 Nov 90 pp 75-78

[Article by V. G. Baryshevskiy, A. G. Davydchenko, M. V. Korzhik, M. G. Livshin, A. S. Lobko, V. I. Moroz, S. A. Smirnova, and A. A. Fedorov]

[Abstract] On account of their better mechanical characteristics and lower manufacturing cost, $YAlO_3:Ce^{3+}$ are considered for use instead of $Gd_2SiO_5:Ce^3$ crystals as high-speed scintillators for measurements of high-intensity nuclear radiations. An experimental study was made for the purpose of optimizing the technology of producing such crystals, namely by growing them by horizontal crystallization in molybdenum containers rather than by vertical pull from iridium crucibles. This technique yielded large crystals, up to 20 mm thick and 100x100 mm^2 wide, with 0.3 wt.% CeO_2 and a perovskite structure. They were tested for density (5.5 g/cm^3), emission wavelength (347 nm), de-excitation time (30 ns), and scintillation efficiency (35 percent). Their absorption spectrum was found to contain two structured bands, with 290 nm and 235 nm center wavelengths respectively, overlapping with the long-wave edge of the fundamental absorption band and related to the $f \rightarrow d$ transitions in Ce^{3+} ions. The effective atomic number of these crystals is 36. Figures 2; tables 1; references 5.

Nature of Exchange Interactions in Uranium Chalcogenides

917J0065A Leningrad FIZIKA TVERDOGO TELA in Russian Vol 32 No 11, Nov 90 pp 3270-3273

[Article by L. G. Chachkhiani, Z. B. Chachkhiani, and M. Yu. Chediya, Georgian Polytechnic Institute imeni V. I. Lenin, Tbilisi]

UDC 669.822.5

[Abstract] It is first explained why known experimental data on uranium chalcogenides U_xS_y, U_xSe_y, and U_xTe indicate nothing else but a dependence of their properties on the chalcogen concentration and of some mean effective exchange interaction on interatomic distances, known models such as the Shubin-Vonsovskiy model of indirect s-d exchange through conduction electrons and the Kramers-Anderson model of indirect superexchange being not generally applicable here. This is so because 5f-electrons, which determine the properties of uranium compounds, are delocalized and the electronics 5f, 6d, 7s bands overlap. Inasmuch as the dependence of their properties on the chalcogen concentration varies appreciably, as the experimental data also indicate, it is proposed that separate consideration of various exchange mechanisms in the self-consistent field approximation and in accordance with the Weiss-Curie law may make each of these models applicable to uranium compounds with a particular chalcogen. This approach implies a disordered distribution of uranium atoms over the chalcogenide crystal structure and, therefore, requires that only data on crystals with known structures be considered so as to avoid any loss of useful information. On the basis of such data, the dependence of the effective exchange integral on the distance between nearest uranium atoms in has been evaluated for compounds with different uranium content (x) in each of the three series of its chalcogenide compounds with S, Se, Te respectively. The effective exchange integral, which determines the magnetic properties of such a compound is, according to the self-consistent field theory, proportional to θ_{pm}/μ_{eff}^2 (θ_{pm} denotes the Curie paramagnetic transition temperature and $\mu_{eff} = C/3K_BN^2$ denotes the effective magnetic moment of a uranium ion, C - Curie constant, K_B - Boltzmann constant, N - Avogadro's number). Calculations of the exchange integral on the basis of these relations and measured paramagnetic susceptibility have yielded a monotonic dependence on the interatomic distance in U-S and U-Se compounds and a nonmonotonic one on the interatomic distance in U-Te compounds. With increasing

interatomic distance, moreover, all exchange integrals have been found to cross from negative to positive through zero at some characteristic for each compound interatomic distance. This contradicts earlier conclusions that exchange through conduction electrons always plays the major role in exchange interactions in such compounds, because all uranium compounds with the same chalcogen have similar structures even when their symmetries are not identical. Only in U-Te compounds do conduction electrons evidently play that major role, while localized p-electrons evidently play that major role in U-S and U-Se compounds. This conclusion implies further that the stability of stoichiometric phases, successfully extracted from U-Te alloys, is associated with the Hume-Rothery stabilization mechanism. Figures 2; references 10.

Excitation Cross-Section of the Isomer U235m in a Plasma, Produced by Electron Beam

917J0066A Moscow YADERNAYA FIZIKA in Russian Vol 53 No 1, Jan 91 pp 36-40

[Article by R. V. Arutyunyan and L. A. Bolshov, Institute of Safety Problems in Development of Atomic Energy, USSR Academy of Sciences, V. D. Vikharev, S. A. Dorshakov, V. A. Kornilo, A. A. Krivovalov, A. A. Smirnov, and Ye. V. Tkalya, Institute of Atomic Energy imeni I. V. Kurchatov, Moscow]

[Abstract] An experimental study has confirmed the feasibility of exciting ^{235}U nuclei from the ground state to an isomer state in a plasma produced as a uranium target is being heated by a relativistic electron beam, such an excitation of ^{235}U nuclei in a plasma produced by surface treatment of natural uranium with a periodically pulsed CO_2 or Neodymium laser having been demonstrated in earlier experiments (Y. Izawa and C. Yamanaka, PHYSICS LETTERS Vol 88B, 1979). This experiment was performed in the TRITON high-current accelerator with a pulsed 150 kA beam of 500 keV electrons, such a beam being generated by voltage pulses of about 30 ns duration. As target were used uranium foils 1.5 mg/cm^2 and 20 mg/cm^2 thick on aluminum substrates 1.6 mg/cm^2 and 10 mg/cm^2 respectively, also uranium ceramic plates 190 mg/cm^2 thick and 6 percent enriched. A target served as the anode of the accelerator diode, uranium vapor from this target-anode vapor being collected by a foil covering the other end of a hollow conical channel-cathode. A steel needle along the axis of this channel-cathode focused the electron beam onto a spot about 2 mm in diameter. After a target had been bombarded with relativistic electrons, the collector with uranium deposit was placed for analysis into a chamber which a BMN-500 molecular pump had evacuated to a residual pressure below 10^{-5} torr. Radioactive decay of the ^{235m}U isomer was monitored by a VEU-6 channel-strip secondary-electron multiplier serving as detector-counter of internal-conversion electrons during de-excitation of isomer nuclei. Its entrance aperture was 15 mm away from the plane of the uranium collector. Its electric output signal was fed through a preamplifier and then a main amplifier to a NOKIA multichannel pulse analyzer, which also recorded the α-spectra. The number of uranium atoms on the collector was counted with the aid of an α-spectrometer. Each uranium target was used 5 - 20 times. An evaluation of the data has confirmed the presence of ^{235m}U nuclei in such a uranium plasma, measurements in all tests except two having yielded a half-life sufficiently close to the known 26 min half-life of this isomer. The results reveal also a linear dependence of the accuracy of recorded decay curves on the degree of electron beam focusing. On the basis of these data and the applicable theoretical relation can be determined the total number N* of isomer ^{235m}U nuclei produced in such a process and thus also the efficiency of the process in terms of the ratio N*/N (N - total number of ^{235}U nuclei. The cross-section for excitation into this isomer under conditions of this experiment has accordingly been estimated at $\sigma_e = 10^{-32} - 10^{-31}$ cm^2. The authors thank V. V. Koltsov and A. A. Rimskiy-Korsakov for supplying the necessary material, D. D. Malyuta and G. A. Polyakov for useful discussion of the results. Figures 3; tables 2; references 10.

Polarization of Neutrons During Diffraction by Magnetized Crystals

917J0066B Moscow YADERNAYA FIZIKA in Russian Vol 53 No 1, Jan 91 pp 41-49

[Article by V. K. Ignatovich and M. I. Podgoretskiy, Joint Institute of Nuclear Research, Dubna, M. I. Tsulaya, Institute of Physics, GSSR Academy of Sciences]

[Abstract] The polarization of thermal neutrons during Bragg scattering of a collimated neutron beam by a magnetized crystal is evaluated, after a preliminary consideration of scattering of a neutron beam with a wide continuous energy spectrum by an unmagnetized perfect crystal with an amosaic structure and by a polyatomic crystal with unit-cell scattering centers. The neutron beam is assumed to impinge on a surface of the crystal parallel to one of its crystallographic planes and the thickness of that crystal is assumed to be larger than the primary-extinction depth for a neutron wave. Neutrons with a momentum component normal to that surface which satisfies the Bragg condition will be reflected, while all other neutrons will enter the crystal. Scattering by a magnetized polyatomic paramagnetic crystal is considered next, the coherent scattering amplitude f being here a function of the scattering angle θ and consisting of two parts: a "magnetic" amplitude A_m proportional to the magnetization of the crystal and a "nuclear" amplitude f_n proportional to the neutron-crystal interaction potential. The "magnetic" amplitude has opposite signs for neutrons polarized parallel to the magnetic field and for neutrons polarized antiparallel to it so that the intensity $J = \alpha|f\theta)$ (α - constant independent of amplitude) of the scattered neutron flux will be

correspondingly different: $J^{up} = \alpha|f_n + f_m|$ and $J_{down} = \alpha|f_n - f_m|$. The total intensity of the entire scattered neutron flux $J_{up} + J_{down}$ is thus either $J = 2\alpha f_m$ and thus depends on the magnetic field H when $f_n < f_m$ or $J = 2\alpha f_n$ and thus does not depend on the magnetic field when $f_n > f_m$. At some magnitude of the magnetic field the two amplitudes become equal, and increasing the magnetic field further will increase the total intensity of the scattered neutron flux. At this magnetic field intensity the derivative dJ/dH passes through a discontinuity, changing stepwise from zero to a positive. There is, therefore, an experimentally verifiable criterion for equality of the two scattering amplitudes $f_n = f_m$ and thus for the possibility of fully polarizing a beam of neutrons, inasmuch as unpolarized incident neutrons acquire a polarization of magnitude $P = (J_{up} - J_{down})/(J_{up} + J_{down})$ as they are being scattered by a magnetized crystal. An energy dispersion of the scattered neutrons due to a dispersion of their angle of incidence does not invalidate the existence of that dJ/dH discontinuity and does not influence the magnitude of the magnetic field at which it occurs because, unlike the intensity of the scattered neutron flux, both scattering amplitudes depend not on the scattering angle but on the momentum transferred during Bragg diffraction. There are three major factors which detract from the exactitude of that polarization criterion. One is the finite thickness of a crystal, the deviation of the dJ/dH discontinuity from the $f_n = f_m$ point increasing with decreasing crystal thickness. Crystals with a mosaic structure are apparently not very effective neutron polarizers when the mosaic blocks are small, and those with large mosaic blocks are in turn not very effective neutron scatterers. The second factor is absorption during incoherent and inelastic scattering, which causes the scattering amplitude to acquire an imaginary component and to thus become a complex quantity. The third factor is the magnetization process, particularly relevant when ferromagnetic crystals are used for polarization of neutrons. Such crystals must have a single-domain structure and therefore need to be strongly magnetized to technical saturation. Additional smooth regulation of f_m to make it equal to f_n may nevertheless be possible because of the available margin from technical saturation to the theoretical maximum saturation, this margin becoming wider as the Curie temperature and thus paramagnetic transition are approached. The anisotropy of the magnetic properties of such crystals has a depolarizing effect. Theoretical estimates for the simplest case of ferromagnetic crystals with only one direction of easy magnetization indicate that this effect is not appreciable. References 11.

Internal Bremsstrahlung Emission During β-Decay into Bound State and Problem of Neutrino Mass

917J0066C Moscow YADERNAYA FIZIKA in Russian Vol 53 No 1, Jan 91 pp 113-116

[Article by I. S. Batkin, T. A. Churakova, and O. V. Shalneva, Voronezh State University]

[Abstract] An experimental method of estimating the neutrino mass is proposed, namely measuring the internal bremsstrahlung emitted during β-decay of a tritium atom and its electron capture into one of the three bound states (1s, 2s, 2p) in the daughter nucleus. The β-transition energy is then divided between two particles, a neutrino and a γ-quantum, while the maximum β-transition energy and thus γ-quantum energy is increased by the electron binding energy. The spectra of internal and external bremsstrahlung emissions have consequently different upper edges, that of internal bremsstrahlung emission being higher. Thus, there exists an energy range of internal bremsstrahlung emission alone and the width of this energy range happens to depend strongly on the neutrino mass. Theoretical validation of this method of estimating that mass is based on an evaluation of that β-decay process in terms of amplitude and probability, following an analysis aided by the applicable Feynman diagram and by expansion of Green's wave function of the electron's intermediate state into multipoles. The form of three spectra of internal bremsstrahlung emission corresponding to electron capture into the 1s-state, the 2s-state, and the 2p-state respectively has been calculated accordingly, in the nonrelativistic approximation, as $dS(\omega)/N_{gb}d\omega = f(\omega)$ (ω - energy of a bremsstrahlung quantum) and thus normalized to the probability of β-transition. The yield of internal bremsstrahlung emission is shown to be higher than its ordinary yield within that energy range only, and restructurization of the electron shell is shown to change the upper edge of its spectrum. Figures 3; references 6.

Nuclear Fusion Induced by Weak Interaction

917J0066D Moscow YADERNAYA FIZIKA in Russian Vol 53 No 1, Jan 90 pp 117-119

[Article by I. S. Batkin and I. V. Kopytin, Voronezh State University]

[Abstract] The feasibility of inducing nuclear fusion reactions other than already known ones such as $p + p \rightarrow d + e^- + \nu_e$ by weak interaction is demonstrated on two specific examples: $n + {}^3H \rightarrow {}^4He + e^- + \nu_e$ and $p + {}^3He \rightarrow {}^4He + e^+ + \nu_e$. The cross-section σ for each reaction is calculated according to the β-decay theory in the $h = c = m_e = 1$ system of units, assuming that the nucleon is captured into the ground state of the ^{4}He isotope and that $g_A/g_V = -1.2$ (g_V denoting the weak-interaction constant). The two nuclear elements of the β-transition matrix $M_V \equiv$ Int 1 and $M_A \equiv$ Int σ are evaluated for the extreme cases of incident nucleons with very low energy ($E_i \leq 1$ eV) and with very high energy ($E_i \geq 1$ MeV), in the approximation of effective scattering length and in the approximation of plane waves respectively. Numerical estimates yield cross-sections $\sigma = 6 \times 10^{-39}$ cm^2 for the first reaction involving an incident 0.04 eV thermal neutron and $\sigma = 5 \times 10^{-44}$ for the second reaction involving an incident 20 MeV proton. References 7.

Applicability of Kramers Formula to Decay of Highly Excited Nuclear Systems

917J0066E Moscow YADERNAYA FIZIKA in Russian Vol 53 No 1, Jan 91 pp 133-141

[Article by I. I. Gonchar and G. I. Kosenko, Omsk Institute of Railroad Transportation Engineers]

[Abstract] Decay of highly excited nuclear systems is analyzed on the basis of Langevin's equations adequately describing the fluctuation-dissipative dynamics of fission (also of fusion), namely fission with fluctuation of internal energy causing temperature fluctuation and with dissipation by friction. The probability current density is accordingly evaluated for systems with a fission barrier B_f lower than the temperature T, following a numerical solution by the Monte Carlo method of those two differential equations which describe the motion of a "Brownian" particle in the one-dimensional model: $d\rho/dt = p/m$ and $dp/dt = -\beta p - \delta V/\delta r + \xi(t)$ (ρ - space coordinate, p - momentum, m - mass, $V(\rho)$ - potential energy, $\beta = \gamma/m$, γ - friction factor, ξ - random force with zero mean, t - time). These two equations are equivalent to the Fokker-Planck equation for the distribution function of collective variables f(r,p,t). As the coordinate of such a particle has been selected half the distance ρ between the centers of mass of subsequent fission fragments, the other degrees of freedom simulating a thermostat. Both mass and friction factor are assumed to be invariable in space. As for the potential energy $V(\rho)$ an S-function has been selected consisting of two parabolas, first descending from a high positive potential to the "ground state" ($V = 0$) on the ρ-axis, then rising to the "barrier height" ($V > 0$), and then again descending to discontinuity ($V < 0$) followed by a descending hyperbola. The two differential equations are converted into difference equations in variables ρ_{n+1} and p_{n+1}, the momentum p_{n+1} at point ρ_{n+1} depending not only on the momentum p_n and the potential gradient $(\delta V/\delta\rho(_n)$ but also on the temperature T_n at point ρ_n. The temperature T, proportional to the square root of internal energy E^*_{int} is calculated after the latter has been determined from the law of energy conservation for each "particle" separately: $E^* = E_{kin} + E^*_{int} + V(\rho)$ (E^* - total excitation energy of nucleus, E_{kin} - kinetic energy of "particle"). Depending on the magnitude of the parameter $\beta' = \beta(m/4C)^{1/2}$, the motion of the system can be underdamped or overdamped. Calculation were made in three ways: 1) initial temperature constant and height of fission barrier B_f varied, 2) height of fission barrier B_f constant and initial temperature varied, 3) initial temperature constant and $B_f = 0$ so that the "ground state" point on the ρ-axis became also the saddle point for two half-parabolas but the "stiffness" C of each half-parabola varied. The results indicate that after probability density current always reaches a quasi-steady limit after a transient period. This limit is shown to be the same as calculated according to Kramers' formula, as long as the fission barrier B_f does not exceed 0.5 MeV. The authors thank Yu. A. Lazarev for interest and helpful discussions, and G. D. Adeyev for constructive critique. Figures 6; references 26.

Spin-Flavor Resonance Precession Amplified by Neutrino Oscillations and Effect on Time Variations of Solar Neutrino Flux

917J0066F Moscow YADERNAYA FIZIKA in Russian Vol 53 No 1, Jan 91 pp 208-214

[Article by Ye. Kh. Akhmedov, Institute of Atomic Energy imeni I. V. Kurchatov]

[Abstract] Experimental data on ^{37}Cl obtained by R. Davis and associates indicate that time variations of the solar neutrino flux take place over an 11 year period within the convective region of the sun, these variations being in an anticorrelation with solar activity. The mechanism of these variations is most likely associated with the magnetic moments of neutrinos. Such a mechanism is shown to be simultaneous resonance spin-flavor precession and resonance flavor oscillation of neutrinos. Considering that the requirement for resonance spin-flavor precession to occur are nonzero nondiagonal in flavor, magnetic moments of neutrinos and thus nonconservation of the lepton flavor, flavor oscillation must then necessarily also take place and both processes need to be regarded as occurring simultaneously. Resonance spin-flavor precession explains those time variations of the solar neutrino flux, if left-to-right neutrino conversion is adiabatic or nearly adiabatic during solar activity and not so during quiescent periods. Depending on the degree of adiabaticity, precession and oscillation will either amplify or attenuate each other when their resonances overlap (Ye. Kh. Akhmedov, ZHURNAL EKSPERIMENTALNOY I TEORETICHESKOY FIZIKI Vol 95, 1989). The overlap of the two resonances widens, moreover, as the neutrino concentration decreases so that their strong interaction within the convective region of the sun, characterized by a low neutrino concentration, is very likely. In the most relevant case of moderate nonadiabaticity, therefore, overlap of the two resonances will make them more nearly adiabatic, inasmuch as both resonances then become wider while both oscillation and precession lengths become smaller. To demonstrate this and thus confirm that time variations of the solar neutrino flux indeed take place, the evolution of a solar ν_{eL} neutrino is analyzed in terms of the probability of its survival on the sun's surface depending on its transient magnetic moment, on the ratio $E/\Delta m^2$ of its energy to its change of mass squared, on its mixing angle, and on the transverse magnetic field under resonance conditions. Numerical estimates for Majorana neutrinos with zero diagonal magnetic moments in a transverse magnetic field with intensity profiles $B_1[0.1/(x + 0.1)]^2$ from $x = 0$ to $x = 0.65$ and $B_0[1 - [x - 0.7)/0.3]^2]$ from $x = 0.65$ to $x = 1$ ($x = r/R_S$, R - radius of sun) indicate that strong amplification of resonance spin-flavor precession and correspondingly wide time variations of the solar neutrino flux in the ^{37}Cl experiment could have occurred, provided the magnetic moments of neutrinos were smaller than $3x10^{-12}\nu_B$. These estimates agree with all existing experimental data, including the Kamiokande II data. Nonresonant spin-flavor precession of neutrinos can, moreover, be

obtained by letting $\Delta m^2 \rightarrow 0$. The author thanks Z. G. Berezhiani, M. I. Vysotskiy, L. B. Okun, and A. Yu. Smirnov for helpful discussions. Figures 3; references 34.

Solitons in Ring Superlattice

917J0067A Tomsk IZVESTIYA VYSSHIKH UCHEBNYKH ZAVEDENIY: FIZIKA in Russian Vol 33 No 11, Nov 90 pp 79-81

[Article by G. M. Shmelev and E. M. Epshteyn, Volgograd Pedagogical Institute]

UDC 621.315.592

[Abstract] Propagation of solitons through a ring superlattice is analyzed, considering a superlattice produced by successive deposition of coaxial parallel annular layers so that they form a stack of pancakes with a center hole. The analysis is based on the one-dimensional Gordon-sine equation in the gauge of a zero scalar potential, which describes the electromagnetic field in a thin superlattice ring. This equation cannot have soliton solutions in the form of solitary "sech" solution, which it can have for a straight superlattice, but it can have soliton solutions in the form of fluxon waves satisfying the condition of periodicity of the electric field. The amplitude E_0 of the electric is related to the angular its angular velocity u and the width w of such a soliton by the equality $u/wE_0 = ed/2h$ (e - electron charge, d - width of superlattice ring, h - Planck's constant). In the limiting case of a ring with an infinite radius this relation reduces to that for a straight superlattice. It is shown that any number of equidistant solitons can propagate through a ring superlattice, according to the fluxon solution, while only either one soliton or an infinite number of them can propagate through a straight one. The axial constant electric field of n solitons in a ring superlattice is calculated, whereupon soliton drag of electrons in such a superlattice is evaluated by utilizing the analogy with a straight superlattice. Numerical estimates of the drag current density are found to be consistent with estimates of charge transferred by a soliton in a straight superlattice. References 7.

Most Simple Emission Electron Microscope for General Physics Research

917J0067B Tomsk IZVESTIYA VYSSHIKH UCHEBNYKH ZAVEDENIY: FIZIKA in Russian Vol 33 No 11, Nov 90 pp 110-111

[Article by L.V. Reshetnikova, N.A. Gorbatyy, and S. Pulatova, Tashkent State University imeni V. I. Lenin]

UDC 53.06

[Abstract] Use of an emission electron microscope operating without a lens as a cylindrical electron projector in laboratory practice is described, a 150-200 mm long tungsten filament 150-200 μm in diameter being a typical object to be examined. The microscope is a 200 mm high glass tube 60-80 mm in diameter placed vertically on an evacuating machine. The filament is fastened inside this tube along its axis, thus also vertically, the inside surface of that tube having been coated with an optically transparent and electrically conductive $SnCl_2$ layer by treatment of the glass with $SnCl_2$ vapor at 400°C. This layer serves as the anode, for thermoelectrons which the filament-cathode emits when connected across the low-voltage secondary of a step-down transformer with the lower terminal grounded, and is put under a high potential of up to 10 kV above ground. The filament temperature is regulated by regulation of its current with an autotransformer. Enlarged images of the filament surface appear on a luminescent coating which has been deposited on that conductive $SnCl_2$ layer and serves as the projection screen. Its material can be ZnS:Cu, ZnS:Ag, or any other cathodoluminophor. It is deposited on either as powder, for which the inside surface of the tube must be first wetted with a binder such as $H_3PO_3 + C_2H_5OH$ or from a powder suspension in acetone with nitrocellulose. The cylindrical screen-anode is placed on a 20-25 mm thick and 50-60 mm in diameter washer made of acrylic glass so as to isolate the conductive layer from the metal stand. For complete degassing of the filament, the latter is heated with electric current up to a maximum temperature within the 2400-2800 K range (bright heat) after the tube has been evacuated to 10^{-5} - 10^{-6} torr. Following this preparation, an emission image of the filament surface is obtained by applying a positive potential of 2-3 kV to the screen-anode and gradually heating the filament from room temperature till the screen will glow when the filament temperature has reached 1700-1800 K. This procedure is designed for completion of all laboratory work, image decoding included, within a 4 h period. In addition to revealing surface defects and contamination as well as crystal growth along a filament, examination with this microscope can also reveal how films of electropositive adsorbates such as alkali metals, alkali-earth metals, and rare-earth metals deposited on a tungsten filament influence its thermoemission power. Figures 2; references 6.

Collective Annihilation of Electron-Positron Plasma in Strong Magnetic Field

917J0071A Moscow ZHURNAL EKSPERIMENTALNOY I TEORETICHESKOY FIZIKI in Russian Vol 99 No 1, Jan 91 pp 127-143

[Article by A. A. Belyanin, V. V. Kocharovskiy, Vl. V. Kocharovskiy, Applied Physics Institute at the USSR Academy of Sciences]

[Abstract] It is shown that the annihilation process in a sufficiently dense e^-e^+-plasma is both collective and coherent in nature and occurs during a considerably shorter time than known noncoherent spontaneous annihilation and collisional relaxation processes. Such a strictly transient process is characterized by correlations within a broad γ-radiation frequency band. It is shown that collective spontaneous annihilation phenomena occur in a dense electron-positron plasma by means of

coherent events of single-photon e^-e^+-pair annihilation in a strong magnetic field (over 10^{13} G). Collective annihilation takes considerably less time to develop than known noncoherent spontaneous annihilation and collisional relaxation processes; it also leads to the excitation of powerful γ-radiation (annihilation superradiance). The collective annihilation (KA) process is due to the instability of normal E-waves within a narrow wave number range near the wave number threshold. In the authors' opinion, the results may serve as the basis for estimating the role of KA among other elementary processes of the dynamics of energy release and dense cosmic and laboratory e^-e^+-plasma decay and emission in strong magnetic fields. The authors are grateful to V. V. Zheleznyakov and Yu. V. Chugunov for discussions and their interest in the effort. References 23: 11 Russian, 12 Western; figures 6.

Polarization Bremsstrahlung Spectrum in Solid Near Absorption Edge

917J0071B Moscow ZHURNAL EKSPERIMENTALNOY I TEORETICHESKOY FIZIKI in Russian Vol 99 No 1, Jan 91 pp 165-167

[Article by V. A. Astapenko, Moscow Engineering Physics Institute]

[Abstract] Polarization bremsstrahlung in solids due to virtual electron transitions (without actually populating intermediate levels) from filled energy bands to empty energy bands, which is especially significant near the absorption band edge in the crystal, is examined. The spectral dependence of the polarization bremsstrahlung of a Born particle near the absorption edge is calculated in a parabolic band approximation. It is shown that a modulation technique can be used in experimental investigations of this radiation. The author is deeply grateful to V. M. Buymistrov for constructive discussion. References 10.

On Topological Interaction of Phonons With Dislocations and Disclinations. II. Scattering Problem

917J0072C Moscow TEORETICHESKAYA I MATEMATICHESKAYA FIZIKA in Russian Vol 86 No 1, Jan 91 pp 81-97

[Article by Ye. M. Serebryanyy, Dnepropetrovsk State University]

[Abstract] Continuation of the author's article in *Teoreticheskaya i matematicheskaya fizika* Vol. 83 No. 3, 1990, pp. 428-446 which shows that in the framework of the linear elasticity theory, there exists a hitherto unknown type of interaction between phonons and linear defects—dislocations and disclinations; the article examined the phenomenon of transition emission of sound in a medium by a source which moves at a constant velocity due to a topological interaction of virtual phonons with defects. The problem of scattering is analyzed in greater detail for transverse and longitudinal phonon modes against the background of a screw dislocation and disclination. The acoustic phonon scattering matrix by linear defects induced by a change in the phonon phase while encircling the defect along a closed path is computed in a continuum limit. It is shown that against the background of a screw dislocation given a negative disclination Frank angle, phonon modes containing components with a kinematic momentum of μ which satisfies the inequality $0 < |\mu| < 1$ are singular. In other words, near the defect line such components may increase infinitely as ρ^{μ} where ρ is the distance to the defect line. General formulae of the scattering matrix and the analysis of the role of singular modes remain valid even in the case where the longitudinal and transverse sound velocities are not equal to each other. In the presence of singular modes, the gauge group curvature concentrated on the defects leads to transitions between different types of polarization. The topological interaction is dominant when the phonon wavelength is much greater than the defect core scattering length by the short-range potential and thus is the most significant in long-range correlation problems. The author is grateful to D. V. Galtsov whose remarks about singular gravitational modes prompted this effort and to S. A. Pritomanov who familiarized the author with the REDUCE language. References 10: 8 Russian, 2 Western; figures 1; tables 1.

Self-Focusing of Relativistic Electron Bunches in Plasma

917J0080B Moscow ZHURNAL EKSPERIMENTALNOY I TEORETICHESKOY FIZIKI in Russian Vol 99 No 2, Feb 91 pp 498-507

[Article by V. G. Dorofeyenko, V. B. Krasovitskiy, Rostov State University imeni M.A. Suslov]

[Abstract] The nonrelativistic theory of electron beam self-focusing in plasma is extended to the relativistic energy domain where beam emission in a plasma is nonpotential and the problem transcends the bounds of electrostatic approximation. A three-dimensional equilibrium of modulated ultrarelativistic electron beams—sequences of electron bunches—in a plasma is examined under self-focusing conditions when the bunch compression by the field generated by the plasma wave beam is balanced by the kinetic pressure gradient in the bunch. Self-focusing of an electron beam broken up into bunches beforehand in a dense plasma occurs when the beam modulation frequency ω_m is less than the plasma frequency ω_p. An analytical solution obtained for random values of $\omega_m < \omega_p$ demonstrates that the drift from the $\omega_m \approx \omega_p$ resonance leads to an elongation of electron bunches given a constant distance between the edges of adjacent bunches and beam radius. The authors are grateful to G. V. Fomin for his help. References 10: 9 Russian, 1 Western; figures 7.

Density of Disordered Solids' Phonon-Fracton States Near Percolation Phase Transitions

917J0080C Moscow ZHURNAL EKSPERIMENTALNOY I TEORETICHESKOY FIZIKI in Russian Vol 99 No 2, Feb 91 pp 530-539

[Article by A. L. Korzhenevskiy, A. A. Luzhkov, Leningrad Electrical Engineering Institute imeni V. I. Ulyanov (Lenin)]

[Abstract] Acoustic properties of disordered solids during percolation phase transitions (FP) with $h \approx 1$ where the parameter h is a ratio of the corresponding constants of different phases is examined in the framework of the field theory approach. An FP with the simplest type of striction interaction for which the solution of the stochastic differential vector equation of elastic medium motion can be reduced to a scalar solution in the critical area is considered. The behavior of elastic effective moduli and the density of phonon-fracton states in the vicinity of percolation phase transitions in elastoisotropic solids is examined by the field renormalization group method. It is shown that the analytical results can be easily extended to other kinetic characteristics, such as effective diffusion coefficient or spin wave rigidity near percolation FP points. The authors are grateful to A. N. Vasilyev, S. L. Ginzburg, and S. V. Maleyev for useful discussions of the issues considered in the article. References 30: 9 Russian, 21 Western.

New Possibilities of Improving Glasses for Integrated Optics

917J0062A Moscow DOKLADY AKADEMII NAUK SSSR in Russian VOl 315 No 2, Nov 90 pp 359-363

[Article by S. K. Yevstropiyev, L. V. Mukhina, G. T. Petrovskiy, corresponding member, USSR Academy of Sciences, and V. D. Khalilev, State Institute of Optics imeni S. I. Vavilov, Leningrad]

UDC 666.11.01:535.21

[Abstract] An experimental study of glasses in the R_2O-R_2O_3-RO_2 class such as nephelin glass for integrated optics was made concerning the feasibility of forming optical ion-exchange waveguide layers which will combine high diffusion stresses with a large optic stress factor. Three such glasses were tested: $25Na_2O$-$25Ga_2O_3$-$50SiO_2$, $25Na_2O$-$25Al_2O_3$-$50GeO_2$, $25Na_2O$-$25Ga_2O_3$-$50GeO_2$. Polished specimens were treated in a KNO_3 melt at 350-500°C temperatures for ion exchange, the length of this treatment being varied from 30 s to 4 h. The refractive index increased as a result of this treatment so that the layers developed into waveguides, the index increment for TM and TE polarization modes depending on the length of treatment time. This dependence is different for each glass, nonmmonotonic with a peak for $25Na_2O$-$25Ga_2O_3$-$50GeO_2$ glass, but indicates that only treatment for certain lengths of time within some range will produce the waveguide effect. This range of treatment time ensuring formation of a waveguide was found not to depend on the treatment temperature but also to be different for TM-mode waveguides and TE-mode waveguides. Also the index profile was found to depend on the treatment time and temperature. The results of tests for TE_0 polarization modes in all three glasses indicate that the maximum attainable increments of the effective refractive index and of birefringence decreases as the treatment temperature is raised. Figures 3; references 15.

Threshold Singularities in Spectrum of Quasiparticles Interacting With Phonons

917J0067C Tomsk IZVESTIYA VYSSHIKH UCHEBNYKH ZAVEDENIY: FIZIKA in Russian Vol 33 No 11, Nov 90 pp 17-20

[Article by N. V. Tkach and V. P. Zharkoy, Chernovitsy State University]

UDC 535.343.2

[Abstract] Free and bound states as well as the ground state into which a system of quasiparticles has been excited by interaction with optical lattice phonons are evaluated within the scope of a one-dimensional model, assuming a quadratic dispersion of the quasiparticles and no dispersion of the phonons. The coupling $\varphi(q)$ is assumed to be constant φ within the actual quasi-momentum range $q_{min} \leq |q| \leq q_{max}$ and zero outside this region. The mass operator $M(k,\omega)$ of such quasiparticles is calculated as their Green's function in the case of multiphonon process. Only the ground state and the lowest two threshold singularities are considered, in the three-phonon approximation and assuming a narrow actual quasi-momentum range. Following a computer-aided solution of the dispersion equation in accordance with all given stipulations, the mass operator was evaluated for a numerical analysis of its dependence on the dimensionless frequency. The results reveal a dependence corresponding to a dispersion equation which has six solutions. The corresponding six energy states are: ξ_1 (excited quasiparticle and one free phonon), ξ_{1c} (bound state of quasiparticle with one phonon), ξ_2 (excited state of quasiparticle and two free phonons), ξ_{2c} and ξ_{3c} (bound states of quasiparticle with two phonons), and ξ_0. Solutions ξ_1, ξ_{1c} determine the pattern of the first threshold singularity and solutions ξ_2, ξ_{2c}, ξ_{3c} determine the pattern of the second threshold singularity. Further calculations have yielded the dependence of all these six energy states on the quasiparticle-phonon interaction intensity (energy), on the width of the actual quasi-momentum range, and on the location of the actual interaction region within the Brillouin zone. The results indicate that with increasing interaction intensity all energy levels shift toward the long-wave region of the spectrum and state ξ_{1c} increasingly separates from state ξ_1, the coupling energy as well as the distance states ξ_{2c} and ξ_{3c} thus also increasing. Figures 2; references 4.

On Kinetics of Diffusion-Controlled Processes on Fractals

917J0071C Moscow ZHURNAL EKSPERIMENTALNOY I TEORETICHESKOY FIZIKI in Russian Vol 99 No 1, Jan 91 pp 295-299

[Article by A. B. Mosol]

[Abstract] Fractal models of amorphous and disordered media which have become popular in recent years are examined. Kinetics of diffusion-controlled reactions described by Smoluchowski's equation for fractal media are analyzed. A class of model potentials is proposed making it possible to find an analytic (quadrature) solution of Smoluchowski's nonstationary equation. Corrections for the standard solution defined by the fractal geometry of the medium are discussed. The effect of long-range potential forces is addressed. In so doing, a particle performing Brownian motion on the fractal in the field of another particle placed at the origin of coordinates is analyzed; for simplicity, a case of spherical symmetry and potential interaction is considered. References 7: 4 Russian, 3 Western.

Light Pressure on Atoms in FM Waves' Field

917J0079A Kiev UKRAINSKIY FIZICHESKIY ZHURNAL in Russian Vol 36 No 2, Feb 91 pp 192-197

[Article by V. S. Voytsekhovich, M. V. Danileyko, A. M. Negriyko, V. I. Romanenko, L. P. Yatsenko, Physics Institute at the Ukrainian Academy of Sciences, Kiev]

UDC 621.373.826

[Abstract] The force acting on an atom in the frequency-modulated waves' field is investigated analytically. A precise expression is derived for the force acting on a two-level atom in the field of a frequency-modulated running wave in the form of a continued fraction. The case of the atom's interaction with two head-on frequency-modulated waves is analyzed numerically in the case of equal intensities. It is shown that the force of stimulated light pressure acting on the atom may noticeably exceed the velocity of spontaneous emission of radiation even in the case where the conditions of adiabatically rapid resonance passage are not met. The radiation frequency modulation makes it possible greatly to expand the range of velocities within which atoms interact effectively with the field. References 9: 6 Russian, 3 Western; figures 2.

Laser Spectroscopy Study of Optical Properties of Liquid Crystals With Stimulated Helicity

917J0079B Kiev UKRAINSKIY FIZICHESKIY ZHURNAL in Russian Vol 36 No 2, Feb 91 pp 239-244

[Article by Ye. D. Belotskiy, I. P. Ilchishin, B. I. Lev, P. P. Tomchuk, M. T. Shpak, Physics Institute at the Ukrainian Academy of Sciences, Kiev]

UDC 532.783

[Abstract] Optical properties of stimulated helical structures of liquid crystals (ZhK) are examined and the relationship between the lasing spectrum of a distributed feedback (ROS) laser and the character of macroscopic liquid crystal molecule ordering in an oriented planar texture is established. Nematic liquid crystals (NZhK) whose helicity was stimulated primarily by an addition of both mesogenic and nonmesogenic optically active dopant (OAD) were investigated. Multi- and single-component liquid crystals were used as matrices. The lasers employed a 10 - 30 μm thick layer of planar NZhK texture with a stimulated swirling helical structure dopant. It is found that these helical structures' selective reflection bands correspond to two director distribution periods which is evident from the laser's two-band emission. Laser spectroscopy data are also confirmed by the presence of two peaks in the nondiffracting polarization transmission spectrum in the stimulated helical structure. A stimulated helical structure model which attributes the presence of the second Bragg frequency in the lasing spectrum to the periodic static soliton arrangement in the ZhK director orientation is proposed. It is shown that the irregular spreading of selective reflection (SO) spectra of the stimulated helical structures is their natural state and is not related to the features of macroscopic ZhK orientation in the planar texture. References 12: 10 Russian, 2 Western; figures 3; tables 1.

Cooling of Plasma Gas by Sound

917J0063C Leningrad PISMA V ZHURNAL TEKHNICHESKOY FIZIKI in Russian Vol 17 No 1, 12 Jan 91 pp 12-14

[Article by A. R. Aramyan, G. A. Galechyan, and A. R. Mkrtchyan, Institute of Application Problems in Physics, Academy of Sciences of Armenian Republic]

[Abstract] An experimental study of sound wave and plasma interaction was made, this interaction having been unexpectedly found to result in appreciable cooling of the plasma gas. Plasma for the experiment was generated by electrical discharge between two stub electrodes 85 cm apart in an argon-filled 100 cm long tube 60 mm in diameter. The tube had been evacuated to a residual air pressure of 0.01 mm Hg before being filled with argon to a pressure of 110 mm Hg. Sound waves in this tube were generated by an acoustic transmitter at one end and received by a microphone at the other end. The frequency of sound waves was 190 Hz, corresponding to a wavelength equal to twice the length of the tube and ensuring formation of standing waves. The temperature of the gas in the discharge region was measured with two thermocouples, one with the junction inside the tube on its axis and one with the junction attached to the tube wall. The sound intensity was varied from zero to 10 relative units while the discharge current was held constant, 90 mA and 60 mA respectively in two series of measurements. As the sound intensity was raised, the initially higher temperature of the gas inside the tube was found to drop while its initially lower temperature at the wall rose and the difference between the two temperatures correspondingly decreased. The gas temperature inside dropped from 433 K to 390 K at a discharge current of 90 mA and from 402 K to 360 K at a discharge current of 60 mA. The gas temperature at the wall rose from 305 K to 335 K and from 308 K to 320 K correspondingly. These results are interpreted on the basis of a temperature-dependent velocity of sound and a parabolic radial temperature profile with a radial temperature gradient dependent on either the pressure at a constant discharge current or on the discharge current at a constant pressure. According to this model, a plane sound wave acquires a front curvature and thus a radial velocity component as it propagates through a discharge tube. The resulting radial motion intensifies the dissipation of heat toward the wall and thus decreases the radial temperature gradient. Figures 1; references 3.

Generating High Pressures in Plana Shock Waves With High-Energy Ion Beams

917J0064C Leningrad PISMA V ZHURNAL TEKHNICHESKOY FIZIKI in Russian Vol 16 No 22, 26 Nov 90 pp 80-85

[Article by O. Yu. Vorbyev, A. L. Ni, and V. Ye. Fortov, Institute of High Temperatures, USSR Academy of Sciences, Moscow]

[Abstract] The feasibility of using an ion beam for accelerating a thin striker and thus generating high-pressure pulses upon impact on a target is examined, on the basis of a numerical experiment involving 3 MeV proton beams of 20 ns pulse duration and following five multilayer targets: A) Au (20 μm thick) + CH_2 (19 μm thick) + Au (5.5 μm thick), B) Al (44.4 μm thick) + CH_2 (40.3 μm thick) + Au (2.5 μm thick), C) Al (44.4 μm thick) + CH_2 (40.3 μm thick) + Al (17.5 μm thick, D) Al (44.4 μm thick) + CH_2 (40.3 μm thick) + Cu (5.3 μm thick), E) Au (20 μm thick) + CH_2 (50 μm thick) + Al (20 μm thick). Calculations were made on the basis of a mathematical model consisting of a closed system of applicable equations of motion for a condensed medium and broad-range semiempirical equations of state, also equations of breakdown kinetics for a continuous medium based on experimentally obtained velocity profiles of a struck free surface and a one-dimensional equation of energy absorption by the target, this being the energy of bound electrons, free electrons, ions, and nuclei. Collective effects and the reverse plasma current were ignored, a beam with a moderate current density below 10 MA/cm^2 being quite defocused. Assuming that the liners for targets A, B, C, D, E had been accelerated over a distance of 500 μm to velocities of 4.03, 5.25, 5.22, 5.25, 8.1 km/s respectively, the pressures generated in these targets should be 2.4, 3.63, 1.16, 2.48, 2.26 Mbar correspondingly. On the basis of these calculations have been plotted pressure, density, and porosity profiles in these targets at various instants of time after impact. Figures 2; tables 1; references 8.

Anomalous Effect of Fluctuations Near Critical States of Plasma

917J0070A Leningrad ZHURNAL TEKHNICHESKOY FIZIKI in Russian Vol 60 No 12, Dec 90 pp 35-42

[Article by V. A. Buts and S. S. Moiseyev, Institute of Space Research, USSR Academy of Sciences, Moscow]

[Abstract] Fluctuations in a plasma owing to randomness of the medium in the presence of an external noise are analyzed, their dispersion increasing and a fluctuation chaos evolving when second moments of the random field increase faster than its first moments. As one example is considered parametric instability following decay of a transverse wave into another transverse one and a Langmuir wave t → t'+ e, in which case fluctuation chaos can exist with amplitudes much smaller than those with which dynamic chaos can and, consequently, new critical states are thus established. The system of three equations for the amplitudes of interacting oscillations is simplified by introduction of a slow exponential new variable, then solved by application of the Furupu-Novikov formula and use of variational derivatives. It was solved numerically for the

nonlinear stage of parametric instability with various values of Γ and Δ. Multiplicative noise is found to play a much larger role than additive noise and randomization can occur also in integrable noiseless systems where dynamic chaos cannot. Fluctuations can moreover accelerate the development of such an instability, multiplicative fluctuations being shown to exponentially accelerate the loss of stability in at least one isolated point and the system then immediately begins passing into a state of intermittent chaos. Another example are charged particles in an external magnetic field with a constant component and a fluctuation component, both components oriented in the same direction, and in the field of a plane electromagnetic wave propagating in the same direction. An analysis of their dynamics in terms of the momentum integral reveals an anomalously strong diffusion of their energy under conditions of self-resonance, close to cyclotron resonance. References 10.

Induced Superconductivity in Superlattice

917J0063B Leningrad PISMA V ZHURNAL TEKHNICHESKOY FIZIKI in Russian Vol 17 No 1, 12 Jan 91 pp 79-83

[Article by G. B. Dubrovskiy, Institute of Engineering Physics imeni A. F. Ioffe, USSR Academy of Sciences, Leningrad]

[Abstract] An experimental study of semiconductor superlattices with minibands in the electronic spectrum was made, SiC crystals belonging in this class of materials. Tests were performed on n-SiC crystals with Schottky barriers. Such a barrier was formed by deposition of a very thin Au or Cr film on the etched crystal face, the electrical resistance of this film being at least 100 Ω. Rhombohedral 15R, 21R, and 27R modifications with a net charge carrier concentration N_d - N_a of the order of 10^{19} cm^3 and an about 10 μm thick space-charge region were selected on the basis of their characteristic coloration. The electrical resistance of that surface barrier was measured at temperatures 77 K and 300 K, with the negative bias current varied over the 0-100 μA range and its frequency varied from 20 Hz to 200 kHz. The results reveal no frequency dependence of the electrical resistance and no Joule-effect heating. The electrical resistance of four out of over 50 specimens had decreased, by as much as 15 - 25 percent at 77 K and by as much 4 - 10 percent at 300 K, as the bias current was increased. Increasing the bias current evidently caused the electrical resistance at some point to "switch" from a higher level to a lower one, this "switch" occurring within the 5-10 μA range at 77 K and within the 30-60 μA range at 300 K. Magnetic field measurements were made with two Au films on opposite faces of the crystal, in special mount with spring-loaded contact tabs for application of the bias voltage. A miniature solenoid producing a magnetic field of 60 Oe and a Hall probe were attached to opposite faces of the crystal. These measurements were also made at temperatures 77 K and 300 K, with the bias current stepwise varied beyond 100 μA. The solenoid was turned on and off on each step, whereupon the magnetic field passing through the crystal was recorded. This magnetic field was becoming weaker in the presence of an external magnetic field, with the solenoid turned on. In the absence of an external magnetic field, with the solenoid turned off, a magnetic field of opposite polarity appeared in the crystal. This indicates a bias-induced anomalous diamagnetism. An analogous "switching" of the magnetic field intensity from a higher level to a lower one was observed in only three out of 40 specimens. No significant difference was detected upon reversal of the direction of the bias current, but the voltage drop was always much larger at the negative barrier, this indicating identical barriers on the C-side and on the Si-side. The author thanks Ye. N. Mokhov for supplying the crystals, A. G. Ostroumov for assistance in the preparation of specimens, V. N. Bogomolov and Ye. K. Kudinov for helpful discussions. Figures 2; references 5.

Dependence of Critical Current for Nb_3Sn Conductor on Number of Strands and on Their Doping

917J0064A Leningrad PISMA V ZHURNAL TEKHNICHESKOY FIZIKI in Russian Vol 16 No 22, 26 Nov 90 pp 22-27

[Article by B. P. Mikhaylov, P. Kovac, P. Hutka, V. S. Kruglov, and T. A. Davlatyan]

[Abstract] An experimental study of Nb_3Sn conductors was made concerning the dependence of the critical current and thus their current-carrying capacity on the number of strands and on the impurity, impurities being added for both accelerating Nb_3Sn layer growth and inhibiting grain growth in the diffusion process during final heat treatment of such a conductor. Conductors with seven strands, with 1615 strands, and single-strand solid cast ones were doped with 0.8 wt.% Zr or with 1.0 wt.% Ti or not doped. All were heat treated at 750°C for a length of time ranging 15 to 75 h. The results confirm that both Zr and Ti, even in such low concentrations, inhibit growth of Nb grains by facilitating formation of oxides and their precipitation as fine particles on the grain boundaries and at the same time raise the Nb recrystallization temperature. These impurities also enhance Nb_3Sn layer growth so that thick (50-100 μm) Nb strands are readily converted into a fine-grain Nb_3Sn phase by a not very long heat treatment. The best were found to be 7-strand Nb_3Sn:Zr conductors, with the critical current density as high as 49.2 kA/cm^2 in a magnetic field of 10 T after diffusion annealing at 750°C for 25 h. Figures 3; tables 1; references 5.

Nonlinear Microwave Response in YBaCuO in Critical State

917J0071D Moscow ZHURNAL EKSPERIMENTALNOY I TEORETICHESKOY FIZIKI in Russian Vol 99 No 1, Jan 91 pp 357-362

[Article by G. I. Leviyev, R. S. Papikyan, M. R. Trunin, Solid State Physics Institute at the USSR Academy of Sciences]

[Abstract] Using the example of the second harmonic generation process, it is shown that the nonlinear YBaCuO response due to the magnetic field in the microwave band can be naturally explained in the framework of Portis's model. The nonlinear YBaCuO response near the T_c is examined experimentally. A nonlinearity mechanism based on the interaction of the superconducting current with free or weakly pinned fluxons is considered, making it possible to describe experimental data. The temperature plot of the second harmonic signal power is explained primarily by the strong dependence of impedance on temperature. In the experiment, a YBaCuO specimen was irradiated by an electromagnetic wave with a given pulse power at a 94 GHz frequency whereby the second harmonic power of the echo signal was measured as a function of various external parameters. The authors are grateful to V. V.

Ryazanov for constructive discussions. References 13: 3 Russian, 10 Western; figures 3.

On Issue of Existence of Superconductivity in Hubbard's Model

917J0072B Moscow TEORETICHESKAYA I MATEMATICHESKAYA FIZIKA in Russian Vol 86 No 1, Jan 91 pp 16-30

[Article by N. N. Bogolyubov, V. A. Moskalenko, Moscow State University and Applied Physics Institute of the Republic of Moldova]

[Abstract] Hubbard's model which describes certain peculiar features of materials with high-T_c superconductivity and Hubbard's single-band model which has a superconducting ground state in the limit of large values of Coulomb's electron repulsion due to second-order magnetic interactions are considered. An alternative version of the theory is proposed in order to establish whether renormalized attraction interaction between electron pairs exists and a superconducting state may form. A generalized Wick theory is suggested for the superconducting phase of Hubbard's single-band model and a thermodynamic diagram technique is developed for taking into account strong electron correlations in the system. An exact Dyson equation is derived for a single-particle correlation Green function and an approximate equation - for the two-particle function. A dynamic system of equations determining the superconducting phase of Hubbard's model is formulated on this basis. Thus, the issue of the existence of a superconducting transition in Hubbard's model on the assumption of a half-populated energy band is reduced to the issue of solving the critical temperature equation. It is shown that superconducting phase cannot be realized on the above assumption. References 10: 6 Russian, 4 Western; figures 2.

Effect of Electron States Hybridization on Critical Temperature of Oxide Superconductors

917J0074A Kharkov FIZIKA NIZKIKH TEMPERATUR in Russian Vol 16 No 12, Dec 90 pp 1518-1523

[Article by V. A. Moskalenko, L. A. Dogotar, M. I. Vladimir, Applied Physics Institute of the Moldovan Academy of Sciences, Kishinev]

UDC 538.945

[Abstract] The effect of hybridization of copper's *d*-orbital and adjacent oxygen's *p*-orbital on the oxide superconductor's critical temperature is examined on the basis of Anderson's periodic model with negative *U*-centers which is used successfully to explain the coexistence of superconductivity and various magnetic states and improve our understanding of the properties of heavy fermions. A generalized canonical Bogolyubov transform for electron operators of Anderson's model is proposed. An equation is derived for defining the critical temperature as a function of the hybridization gap, renormalized localized state energy on a paramagnetic assumption, and the corresponding energy bandwidth which is relevant to superconductivity. The critical value of the hybridization gap at which $T_c = 0$ is found. The mean field method is used to describe the two-particle interaction processes in order to examine the effect of hybridization on the development of superconductivity. References 13: 4 Russian, 9 Western.

Abnormal YBaCuO Film Response to Superweak Magnetic Fields

917J0074B Kharkov FIZIKA NIZKIKH TEMPERATUR in Russian Vol 16 No 12, Dec 90 pp 1524-1530

[Article by A. M. Grishin, V. F. Drobotko, D. G. Yemelyanenkov, Yu. N. Inkin, I. V. Nikonets, V. A. Khokhlov, Donetsk Engineering Physics Institute at the Ukrainian Academy of Sciences]

UDC 538.945

[Abstract] The technique for recording the diamagnetic response of submicrometer high-T_c (VTSP) films in weak magnetic fields is refined. The diamagnetic response of 0.8 μm thick and 76 mm wide $YBa_2Cu_3O_{7-x}$ films obtained by the method of DC magnetron sputtering with the help of a standard "Oratoriya-5" unit near the superconductor critical temperature is examined as a function of the AC exciting magnetic field amplitude. A composite Y-Ba-Cu target was used. The film was a granulated medium with a broad $\Delta \approx 50$K transition on the plot of resistance vs. temperature. It is established that in the domain of superweak magnetic fields of 0.1 - 5 mOe, hysteresis losses decrease sharply, so the line of dissipative losses has a fine structure. A peak in AC susceptibility with an increase in the AC magnetic field amplitude shifts to lower temperatures by a given law. The magnetic flux penetration differs from the critical state model. Diamagnetic screening decreases with a decrease in magnetic field. References 12: 5 Russian, 7 Western; figures 4.

Magnetoresistance Anomaly of High-T_c Superconducting Perovskites

917J0074C Kharkov FIZIKA NIZKIKH TEMPERATUR in Russian Vol 16 No 12, Dec 90 pp 1592-1595

[Article by A. M. Glukhov, I. M. Dmitriyenko, A. S. Pokhila, N. Ya. Fogel, Engineering Physics Institute of Low Temperatures at the Ukrainian Academy of Sciences, Kharkov]

UDC 538.945

[Abstract] Characteristic features of resistive transitions of metal oxide perovskites in the magnetic field which do not fit the pattern of the usual fluctuation behavior at T T_c and may, in the authors' opinion attest to the contribution of individual superconducting CuO planes or chains virtually not coupled by interaction are analyzed. The position of the "fixed" point on the resistance vs. temperature plot of polycrystal and single crystal $YBa_2Cu_3O_x$ films which separates two resistive transition areas measured in different magnetic fields is examined. In one of the areas, resistance is only slightly sensitive to the magnetic field strength. It is shown that the fixed point position does not depend on the magnetic field and attests to a weak effect of the magnetic field on resistance near T_c. It is found that the type of resistive transition in superconducting perovskite resembles a percolation transition more than a second-kind regular phase transition. The anomalous dependence of resistance on temperature is attributed to the considerable T_c inhomogeneities and the contribution of single CuO planes to a decrease in resistance; the planes display fluctuation superconductivity but are not coupled by Josephson's interaction. The authors are grateful to L. I. Glazman and R. I. Shekhter for discussing the results. References 4; figures 3.

Upper Critical Field of Bipolaron Superconductors

917J0080D Moscow ZHURNAL EKSPERIMENTALNOY I TEORETICHESKOY FIZIKI in Russian Vol 99 No 2, Feb 91 pp 574-588

[Article by A. S. Aleksandrov, D. A. Samarchenko, Moscow Engineering Physics Institute]

[Abstract] A method which makes it possible to determine the temperature dependence of the upper critical field for a spatially homogeneous state of a bipolaron system is presented allowing for crystal anisotropy. This state is attained for a weak dynamic interaction at a random bipolaron concentration or at a low concentration. It is found that even without dynamic interaction between the particles, the field is nonzero due to the kinematic interaction which appears due to bipolaron commutation relations. In narrow-band crystals with a strong electron-phonon interaction, electrons form site-localized coupled pairs or small-radius bipolarons. It is shown that their properties can be described with the help of an equivalent Bose Hamiltonian given any concentration. The unusual behavior of this field in high-T_c semiconductors is explained on the basis of the resulting dependence. It is noted that the unusual temperature dependence was observed earlier in a low temperature anisotropic metal oxide crystal. References 27: 6 Russian, 21 Western; figures 7.

On Basic Principles of Relativistic Theory of Gravity

917J0072A Moscow TEORETICHESKAYA I MATEMATICHESKAYA FIZIKA in Russian Vol 86 No 1, Jan 91 pp 3-15

[Article by A. A. Logunov, M. A. Mestvirishvili, Moscow State University]

[Abstract] The general theory of relativity (OTO) is analyzed showing that acceptance of its concept violates the laws of preservation of energy and momentum and moment of momentum of matter and gravitational field as well as a notion that the gravitational field is a classical Faraday-Maxwell field. The relativistic theory of gravity (RTG) is explained more systematically than in the authors' 1989 book (Relyativistskaya teoriya gravitatsii. Moscow: Nauka); special attention is focused on the gauge group analysis. For illustration, it is shown that while the OTO is incapable of answering the question of the radio signal delay in the sun's filed, the RTG is perfectly capable of doing so by incorporating Minkovskiy's metric tensor of space. Minkovskiy's space is defined as a fundamental space for all physical fields, including the gravitational (in pseudo-Euclidean geometry of space-time). The gravitational field is described by a symmetric second-rank tensor and is defined as a real physical field with a density of energy momentum. References 7.

New Approach to Boussinesq's and Cherruti's Problems for Elasticity Theory System

917J0075A Moscow VESTNIK MOSKOVSKOGO UNIVERSITETA: MATEMATIKA, MEKHANIKA in Russian No 1, Jan-Feb 91 pp 12-23

[Article by V. A. Kondratyev, O. A. Oleynik]

UDC 517.9

[Abstract] Boundary value problems for a system of equations of the theory of elasticity pointed out to the authors by I. Sneddon are considered. Formulations of these problems date back to works of J. Boussinesq (1885) and V. Cherruti (1882). The theorem of existence and uniqueness of solutions of these boundary value problems is proven on the basis of Korn's and Hardy's inequalities in unbounded domains in classes of vector functions with a finite energy or finite Dirichlet integral. Classical boundary value problems in a half-space are examined for a stationary system of equations of the theory of elasticity with variable coefficients. It is shown that these solutions are stable to changes on the right sides of the system. References 6: 2 Russian, 4 Western.

NTIS
ATTN: PROCESS 103

5285 PORT ROYAL RD
SPRINGFIELD, VA 22161

Foreign Broadcast Information Service (FBIS) and Joint Publications Research Service (JPRS) publications contain political, military, economic, environmental, and sociological news, commentary, and other information, as well as scientific and technical data and reports. All information has been obtained from foreign radio and television broadcasts, news agency transmissions, newspapers, books, and periodicals. Items generally are processed from the first or best available sources. It should not be inferred that they have been disseminated only in the medium, in the language, or to the area indicated. Items from foreign language sources are translated; those from English-language sources are transcribed. Except for excluding certain diacritics, FBIS renders personal and place-names in accordance with the romanization systems approved for U.S. Government publications by the U.S. Board of Geographic Names.

Headlines, editorial reports, and material enclosed in brackets [ ] are supplied by FBIS/JPRS. Processing indicators such as [Text] or [Excerpts] in the first line of each item indicate how the information was processed from the original. Unfamiliar names rendered phonetically are enclosed in parentheses. Words or names preceded by a question mark and enclosed in parentheses were not clear from the original source but have been supplied as appropriate to the context. Other unattributed parenthetical notes within the body of an item originate with the source. Times within items are as given by the source. Passages in boldface or italics are as published.

SUBSCRIPTION/PROCUREMENT INFORMATION

The FBIS DAILY REPORT contains current news and information and is published Monday through Friday in eight volumes: China, East Europe, Soviet Union, East Asia, Near East & South Asia, Sub-Saharan Africa, Latin America, and West Europe. Supplements to the DAILY REPORTs may also be available periodically and will be distributed to regular DAILY REPORT subscribers. JPRS publications, which include approximately 50 regional, worldwide, and topical reports, generally contain less time-sensitive information and are published periodically.

Current DAILY REPORTs and JPRS publications are listed in *Government Reports Announcements* issued semimonthly by the National Technical Information Service (NTIS), 5285 Port Royal Road, Springfield, Virginia 22161 and the *Monthly Catalog of U.S. Government Publications* issued by the Superintendent of Documents, U.S. Government Printing Office, Washington, D.C. 20402.

The public may subscribe to either hardcover or microfiche versions of the DAILY REPORTs and JPRS publications through NTIS at the above address or by calling (703) 487-4630. Subscription rates will be provided by NTIS upon request. Subscriptions are available outside the United States from NTIS or appointed foreign dealers. New subscribers should expect a 30-day delay in receipt of the first issue.

U.S. Government offices may obtain subscriptions to the DAILY REPORTs or JPRS publications (hardcover or microfiche) at no charge through their sponsoring organizations. For additional information or assistance, call FBIS, (202) 338-6735,or write to P.O. Box 2604, Washington, D.C. 20013. Department of Defense consumers are required to submit requests through appropriate command validation channels to DIA, RTS-2C, Washington, D.C. 20301. (Telephone: (202) 373-3771, Autovon: 243-3771.)

Back issues or single copies of the DAILY REPORTs and JPRS publications are not available. Both the DAILY REPORTs and the JPRS publications are on file for public reference at the Library of Congress and at many Federal Depository Libraries. Reference copies may also be seen at many public and university libraries throughout the United States.